Flexibility and Function in HIV Protease: Dynamics of the HIV-1 Protease Bound to the Asymmetric Inhibitor Kynostatin 272 (KNI-272)

ARTICLE *in* JOURNAL OF THE AMERICAN CHEMICAL SOCIETY · JULY 1998

Impact Factor: 12.11 · DOI: 10.1021/ja981206r

7 AUTHORS, INCLUDING:

Darón I Freedberg
U.S. Food and Drug Administration
52 PUBLICATIONS **1,575** CITATIONS
SEE PROFILE

Stephen J Stahl
U.S. Department of Health and Human Services
121 PUBLICATIONS **7,202** CITATIONS
SEE PROFILE

Flexibility and Function in HIV Protease: Dynamics of the HIV-1 Protease Bound to the Asymmetric Inhibitor Kynostatin 272 (KNI-272)

Darón I. Freedberg,[†] Yun-Xing Wang,[†] Stephen J. Stahl,[§] Joshua D. Kaufman,[§] Paul T. Wingfield,[§] Yoshiaki Kiso,[‡] and Dennis A. Torchia*,[†]

Contribution from the Molecular Structural Biology Unit, National Institute of Dental Research, National Institutes of Health, Bethesda, Maryland 20892, National Institute of Arthritis and Musculoskeletal and Skin Diseases, Bethesda, Maryland 20892, and Kyoto Pharmaceutical University, Yamashina-Ku, Kyoto 607, Japan

Received April 9, 1998

Abstract: The HIV-1 protease is a 22 kDa homodimeric protein essential for function of the AIDS virus, and protease inhibitors have been developed into effective HIV drugs. In order to better understand HIV-1 protease−inhibitor interactions, we have investigated amide backbone dynamics by correlated $^{1}H-^{15}N$ NMR spectroscopy. To date, HIV-1 protease/inhibitor complexes studied by NMR spectroscopy have been limited to C_2 symmetric structures, consisting of the protease bound to a symmetric inhibitor. Herein we report studies of the dynamics of HIV-1 protease complexed to KNI-272, a potent (K_i ca. 5 pM), *asymmetric* inhibitor which lifts the chemical shift degeneracy of the protease monomers and allows us to ascertain if the individual protease monomers have significantly different backbone motions. Using isotope filtered/edited spectra of $^{15}N/^{13}C$ protease complexed with unlabeled KNI-272, together with distances derived from the protease/KNI-272 X-ray structure, we obtained monomer specific NMR signal assignments. We derived information about monomer dynamics from a Lipari-Szabo analysis of amide ^{15}N T_1, T_2, and NOE values. Modeling the complex as an axially symmetric rotor yielded an average overall correlation time of 9.65 ns and an anisotropy, $D_{||}/D_{\perp}$, of 1.27. Over 90% of the backbone amide sites are highly ordered with the squared order parameter, averaged over all measured residues, being 0.85. High amplitude internal motions are observed in several loops in the protease, especially those in the elbows of the flaps, while millisecond to microsecond time scale motion is observed at the flap-tips. While these results are similar to those reported for complexes with symmetric inhibitors, we find differences in internal motions between several residues in the flap of one monomer and the corresponding residues on the other monomer. Residue Gly 149 has a significantly larger order parameter than Gly 49; in addition, the motions on the chemical exchange time scale contribute to the relaxation of Gly 152 and Phe 153 but not to the relaxation of Gly 52 and Phe 53. These differences in flexibility correlate with differences in interactions made by these residues with KNI-272, as seen in the crystal structure. We also find that the average of the order parameters measured for residues in monomer 1 is less than for monomer 2, a result that correlates with the observation that average *B* factor for these residues is less in monomer 2 than in monomer 1.

Introduction

Recently, the FDA approved compounds which inhibit the Human Immunodefficiency Virus protease (HIV-Pr) and effectively treat HIV infected individuals. HIV-Pr processes the Gag and Pol polyproteins into mature structural proteins and enzymes which are required in the viral lifecycle.[1,2] HIV-Pr inhibitors inactivate the protease by binding tightly at its catalytic site, resulting in the production of immature, noninfectious viral particles.[3] In clinical trials HIV-Pr inhibitors have decreased the amount of virions (HIV) in blood by as much as 99%,[4,5] but in order to minimize the creation of protease−inhibitor resistant mutants, these new drugs have been used in combination with reverse-transcriptase inhibitors. Not only has combination therapy reduced viral loads in HIV-positive patients but also it has increased their CD4 cell counts.[4,5]

Because HIV-Pr inhibitors play a crucial role in controlling AIDS, a detailed understanding of protease/inhibitor interactions remains of great interest in order to further improve drug design. The protease is a homodimer (whose monomers are numbered 1−99 and 101−199 herein, for monomer 1 and monomer 2, respectively), and X-ray studies have shown that the flaps of the inhibited enzyme (residues 46−56 and 146−156)[6] are closed over the inhibitor and are linked to the inhibitor by a network of hydrogen bonds involving bridging water molecule or water

* Corresponding author: e-mail torchia@yoda.nidr.nih.gov.
[†] National Institute of Dental Research, National Institutes of Health.
[§] National Institute of Arthritis and Musculoskeletal and Skin Diseases, National Institutes of Health.
[‡] Kyoto Pharmaceutical University.

(1) Huff, J. R. *J. Med. Chem.* **1991**, *34*, 2305−2314.
(2) Debouck, C. *AIDS R. H.* **1992**, *8*, 153−164.
(3) Kohl, N. E.; Emini, E. A.; Schleif, W. A.; Davis, L. J.; Heimbach, J. C.; Dixon, R. A. F.; Scolnick, E. M.; Sigal, I. S. *Proc. Natl. Acad. Sci. U.S.A.* **1988**, *85*, 4686−4690.
(4) Wei, X.; Ghosh, S. K.; Taylor, M. E.; Johnson, V. A.; Emini, E. A.; Deutsch, P.; Lifson, J. D.; Bonhoeffer, S.; Nowak, M. A.; Hahn, B. H.; Saag, M. S.; Shaw, G. M. *Nature* **1995**, *373*, 117−122.
(5) Richman, D. D. *Nature* **1995**, *374*, 494.

S0002-7863(98)01206-2 CCC: $15.00
Published on Web 07/25/1998

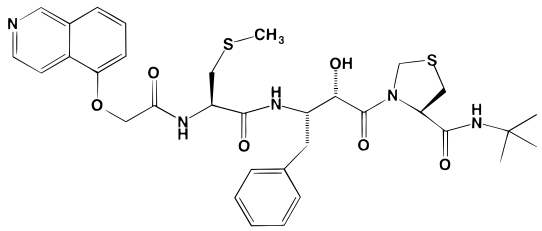

Figure 1. The chemical structure of KNI-272. When this asymmetric molecule binds to the protease, signals of corresponding residues (residues i and i + 100) in the two monomers, particularly those near the inhibitor binding site, often have distinct chemical shifts. Differences in crystallographic *B*-factors were also found for some of these residues in the crystal structure of the HIV-Pr/KNI-272 complex[39] suggesting that there may be differences in the flexibility of the two monomers at the inhibitor binding site of the protease.

molecule mimic. A variety of experimental[6,7] and theoretical studies[8−10] indicate that flexibility of the protease flaps permits access to the active site and is therefore important for function. Nuclear magnetic resonance (NMR) spectroscopy is well suited to study molecular dynamics because NMR relaxation parameters are sensitive to molecular motions covering a time scale ranging from ps to ms.[11] Previous studies[12,13] showed that the flap-elbows, residues 37−42/137−142, are flexible when HIV-Pr is bound to the symmetrical inhibitors DMP323 and P9941 ($K_i = 0.27$ and 9 nM, respectively). These studies also provided evidence for conformational exchange on the microsecond (μs) time scale for residues at the tips of the flaps at 35 °C.[12] Although backbone order parameters of individual amide sites in the DMP323 and P9941 complexes are nearly the same, the protease Gly 48/148 order parameter is roughly 20% smaller in the DMP323 complex than in the P9941 complex. This observation was attributed to the lack of an NH hydrogen bond acceptor in the HIV-Pr/DMP323 complex, imparting greater flexibility to Gly 48/148 in the DMP323 complex.

The above results illustrate that even when two complexes have similar dynamics at nearly all backbone amide sites, significant local differences in flexibility, reflecting differences in specific HIV-Pr-inhibitor interactions, can nonetheless be observed. In the crystal structure of the protease complexed with KNI-272[14] (Figure 1), an asymmetric but highly potent inhibitor ($K_i = 5.5$ pM) of the protease,[15] variations in *B* factors suggest that the inhibitor interacts differently with the two monomers. Although the two monomers cannot be differentiated in NMR spectra of HIV-Pr complexes with symmetrical inhibitors (e.g., DMP323, $K_i = 0.27$ nM, and P9941, $K_i = 9$ nM),[12] the chemical shifts of the two monomers are distinct in the $^1H-^{15}N$ HSQC spectrum of the HIV-Pr/KNI-272 complex. This observation implies that if KNI-272 interacts differently with the two monomers, we may be able to observe differences in their local, and perhaps overall, internal flexibility. The identification of flexible protease sites may point to specific inhibitor sites where changes in inhibitor design could improve drug potency.

Theory

The relationship between molecular reorientation and nuclear spin relaxation makes it possible to obtain quantitative information about amplitudes and time scales of motions within proteins from an analysis of relaxation measurements.[11] Amide ^{15}N relaxation times are particularly well suited to investigate protein backbone dynamics.[16−18] At 500 MHz, the major relaxation mechanism of an ^{15}N amide spin is dipolar relaxation by the directly bonded hydrogen nucleus, with a smaller contribution from ^{15}N chemical shift anisotropy, CSA, relaxation.[16] Longitudinal relaxation times, T_1's, transverse relaxation times, T_2's, and the nuclear Overhauser effect, NOE, of the amide nitrogens are related by eqs 1−3 to the spectral density functions, $J(\omega)$, that contain information about NH bond reorientation. In the

$$\frac{1}{T_1} = \frac{d^2}{10}\left[\left(J(\omega_N - \omega_H) + 3J(\omega_N)\left(1 + \frac{c^2}{3d^2}\right) + 6J(\omega_N + \omega_H)\right)\right] \quad (1)$$

$$\frac{1}{T_2} = \frac{d^2}{20}\left(\left(1 + \frac{c^2}{3d^2}\right)(4J(0) + 3J(\omega_N)) + 6J(\omega_H) + J(\omega_N - \omega_H) + 6J(\omega_N + \omega_H)\right) + R_{ex} \quad (2)$$

$$\mathrm{NOE} = 1 + \left[\frac{\gamma_H}{\gamma_N} d^2(6J(\omega_N + \omega_H) - J(\omega_N - \omega_H))T_1\right] \quad (3)$$

above equations, $d = \hbar\gamma_H\gamma_N/r^3_{N-H}$, $c = (\gamma_N B_0 \Delta\sigma)$, γ_H and γ_N are the respective proton and nitrogen magnetogyric ratios, r_{N-H} is the nitrogen−hydrogen bond length, taken here to be 1.02 Å, $\Delta\sigma$ is the ^{15}N chemical shift anisotropy, −160 ppm,[19] and R_{ex} is the exchange contribution to the line width. A fourth relaxation parameter, $T_{1\rho}$, the longitudinal relaxation time in the rotating frame, is also related to $J(\omega)$ by eq 2, although the explicit form for R_{ex} is different for T_2 and $T_{1\rho}$.[20] It has been pointed out that it is more straight forward to correct $T_{1\rho}$ measurements for off resonance effects, than T_2 measurements.[13,21,22]

The model-free formalism of Lipari and Szabo[23,24] provides a connection between $J(\omega)$ and parameters that describe internal

(6) Wlodawer, A.; Erickson, J. W. *Annu. Rev. Biochem.* **1993**, *62*, 543−585.
(7) Freedberg, D. I.; Torchia, D. A. Unpublished results.
(8) Collins, J. R.; Burt, S. K.; Erickson, J. W. *Nat. Struct. Biol.* **1995**, *2*, 334−338.
(9) Harte, W. E.; Swaminathan, S.; Beveridge, D. *Prot. Struct. Funct. Genet.* **1992**, *13*, 175−194.
(10) Harte, W. E.; Swaminathan, S.; Mansuri, M. M.; Martin, J. C.; Rosenberg, I. E.; Beveridge, D. L. *Proc. Natl. Acad. Sci. U.S.A.* **1993**, *87*, 8864−8868.
(11) Abragam, A. *Principles of Nuclear Magnetism*; Oxford University Press: New York, 1961.
(12) Nicholson, L. K.; Yamazaki, T.; Torchia, D. A.; Grzesiek, S.; Bax, A.; Stahl, S. J.; Kaufman, J. D.; Wingfield, P. T.; Lam, P. Y. S.; Jadhav, P. K.; Hodge, C. N.; Domaille, P. J.; Chang, C. W. *Nat. Struct. Biol.* **1995**, *2*, 274−280.
(13) Tjandra, N.; Wingfield, P. T.; Stahl, S. J.; Bax, A. *J. Biomol. NMR* **1996**, *8*, 273−284.
(14) Mimoto, T.; Imai, J.; Kisanuki, S.; Enomoto, H.; Hattori, N.; Akaji, K.; Kiso, Y. *Chem. Pharm. Bull.* **1992**, *40*, 2251−2253.
(15) Humphrey, R. W.; Nguyen, B.-Y.; Wyvill, K. M.; Shay, L. E.; Lietzau, J.; Ueno, T.; Fukasawa, T.; Hayashi, H.; Mitsuya, H.; Yarchoan, R. *A Phase I Trial of HIV Protease Inhibitor KNI-272 In Patients with AIDS or Symptomatic HIV Infection*; Humphrey, R. W., Nguyen, B.-Y., Wyvill, K. M., Shay, L. E., Lietzau, J., Ueno, T., Fukasawa, T., Hayashi, H., Mitsuya, H., Yarchoan, R., Eds.; Vancouver, BC, 1996; Vol. Mo.B., p 77.
(16) Kay, L. E.; Torchia, D. A.; Bax, A. *Biochemistry* **1989**, *28*, 8972−8979.
(17) Kördel, J.; Skelton, N. J.; Akke, M.; Palmer, A. G.; Chazin, W. J. *Biochemistry* **1992**, *31*, 4856−4866.
(18) Barbato, G.; Ikura, M.; Kay, L. E.; Pastor, R. W.; Bax, A. *Biochemistry* **1992**, *31*, 5269−5278.
(19) Hiyama, Y.; Niu, C.-H.; Silverton, J.; Bavoso, A.; Torchia, D. A. *J. Am. Chem. Soc.* **1988**, *110*, 2378−2383.
(20) Peng, J.; Thanabal, V.; Wagner, G. *J. Magn. Reson.* **1991**, *95*, 421−427.
(21) Davis, D. G.; Perlman, M. E.; London, R. E. *J. Magn. Reson.* **1994**, *B 104*, 266−275.
(22) Ross, A.; Czisch, M.; King, G. C. *J. Magn. Reson.* **1997**, *124*, 355.

motions of NH bonds, without the need to assume a specific model for such motions. In its simplest form, this formalism assumes that the overall motion of the protein is isotropic and characterized by a single correlation time, τ_c. If the correlation times for the internal motions of the NH bond vector are much smaller than τ_c, the model-free approach shows that[23,24]

$$J(\omega) = \frac{2}{5}\left(\frac{S^2\tau_c}{1+(\omega\tau_c)^2} + \frac{(1-S^2)\tau}{1+(\omega\tau)^2}\right) \quad (4)$$

Here, $1/\tau = 1/\tau_c + 1/\tau_e$, where τ_e is the effective correlation time of the internal motion and S is the generalized order parameter which contains information about the spatial extent of NH bond motion. When the internal motion of the NH bond is isotropic $S^2 = 0$, and in the absence of internal motion $S^2 = 1$.

While relaxation data for most residues can usually be fitted using the two model free parameters and τ_c, it is sometimes necessary to include a nonzero R_{ex} contribution to $1/T_2$ or to $1/T_{1\rho}$ (see eq 2) in order to account for transverse relaxation caused by chemical exchange (that is, motion on the ms-μs time scale that modulates the isotropic chemical shift). Alternatively, it may be necessary to use the extended model-free formulation to fit the relaxation data. This formalism uses two order parameters, S_f^2 and S_s^2, to account for "fast" (ps) and "slow" (ns) internal motions.[25]

Theoretical[26] and experimental[13,27,28] studies show that interpretation of additional parameters, such as R_{ex} or S_f and S_s, in the model-free approach should be carried out with caution, particularly when the assumption of isotropic reorientation is not justified. Even when overall reorientation is only slightly anisotropic (i.e., $(D_{||}/D_\perp) < 1.4$, where $D_{||}$ and $D_\perp$ are the respective rotational diffusion constants parallel and perpendicular to the long axis of a symmetric rotor), it is important to apply the anisotropic analysis. Otherwise it may be necessary to use either a nonzero R_{ex} value or two order parameters, S_s and S_f (extended model-free treatment) to fit relaxation data[13,27] to compensate for the neglect of anisotropic overall motion. Recently, the model-free formalism was used to extract order parameters and internal correlation times of anisotropically tumbling molecules.[13,23,24,27,29,30] For an axially symmetric rotor, $J(\omega)$ is given by[27]

$$J(\omega) = \sum_{k=1}^{3} A_k\left(\frac{S^2\tau_k}{1+(\omega\tau_k)^2}\right) + \frac{(1-S^2)\tau}{1+(\omega\tau)^2} \quad (5)$$

where $A_1 = (3/2\cos^2\alpha - 1/2)^2$, $A_2 = 3\sin^2\alpha\cos^2\alpha$, and $A_3 = 3/4\sin^4\alpha$, α is the angle the N−H bond vector makes with the unique diffusion axis, $\tau_1 = (6D_\perp)^{-1}$, $\tau_2 = (D_\perp + 5D_{||})^{-1}$, $\tau_3 = (4D_\perp + 2D_{||})^{-1}$, $1/\tau = (1/\tau_e + 1/\bar{\tau})$, $1/(6\bar{\tau}) = D$, $D = (D_{||} + 2D_\perp)/3$, and $\tau_e \ll \bar{\tau}$. A straight forward application of Woessner's equations[29,30] shows that

$$T_2/T_1 \approx (T_2/T_1)_{\alpha=0}(1 + \epsilon\sin^2\alpha) \quad (6)$$

where $\epsilon = (D_{||}/D_\perp - 1)$. Numerical simulations show that eq 6 is a useful approximation (error in $D_{||}/D_\perp$ less than 10%) when $(\omega\tau_1)^2 \gg 1$ and $1 \le D_{||}/D_\perp \le 2.2$. Equation 6 is essentially the reciprocal of eq 15 of Lee et al.[31] We plot T_2/T_1 as a function of $\sin^2\alpha$, because this ratio remains a linear function of $\sin^2\alpha$ for larger values of ϵ than does T_1/T_2.

Materials and Methods

Protein Expression and NMR Sample Preparation. We previously described the preparation of HIV-Pr (strain HXB2), containing cysteine to alanine mutations at positions 67 and 95 and the HIV-Pr/KNI-272.[32] We dissolved the HIV-PR/KNI-272 complex in a 50 mM sodium acetate buffer, pH 5.2, in 95% H_2O/5% D_2O, and recorded relaxation measurements on a 0.7 mM sample in a Shigemi microcell (Allison Park, PA), volume = 230 μL, with the top tightly wrapped with Teflon tape then Parafilm. We measured H/D exchange on a sample in a Wilmad tube (Buena, NJ), volume = 420 μL, wrapped with Parafilm; we exchanged the protein into a D_2O buffer (pD = 5.2, uncorrected) at 5 °C in a Centricon 10 (amicon, Beverly, MA). After exchange, we kept the sample at 5 °C for ca. 15 min and then inserted into the NMR probe at 34 °C. We began data acquisition 10 min later, at which time thermal equilibrium was attained in the probe.

Nuclear Magnetic Resonance Measurements. We measured T_1, T_2, and NOE on a Bruker AMX500 spectrometer using a triple resonance probe equipped with a shielded z gradient coil. We recorded spectra at resonance frequencies of 50.68 and 500.13 MHz, using 90° pulses of 48 and 7.9 μs applied at 117.0 and 4.69 ppm, for ^{15}N and ^{1}H, respectively, with 768 complex points in the ^{1}H dimension and 150 complex points in the ^{15}N dimension. We acquired 40 and 48 scans per complex t1 point for T_1 and T_2 spectra, respectively, and collected two relaxation data sets for each parameter using previously published pulse sequences,[33,34] modified with pulsed-field z-gradients.[33,34] We used recovery delays of 32, 80, 160, 200, 400, 640, 960, and 1360 ms and 32, 48, 80, 128, 272, 400, 720, and 960 ms to measure ^{15}N T_1 values and delay times of 8, 16, 32, 48, 80, 112, 144, and 176 ms and 8, 16, 24, 40, 64, 80, 96, and 144 ms to measure ^{15}N amide T_2 values. The period between the centers of the 180° CPMG pulses was 1 ms in the T_2 experiments. Using the equations of ref 22, together with our acquisition parameters, we calculate that the maximum error in T_2 caused by the ^{15}N resonance offset effect is less than 1.5%. A second resonance offset effect is caused by the different relaxation rates of the tranverse and longitudinal components of the ^{15}N magnetization generated during the CPMG 180° pulses. This causes our measured T_2 values to be overestimated by an average of 2%. We did not correct for this effect because it has only a minor impact, ca. 1%, on the derived values of the overall correlation times and order parameters. More significantly, it has negligible impact on the differences in S^2, since the effective resonance offset is nearly the same for residues i and i + 100 in the two monomers.

We processed the spectra with Lorentz-to-Gauss functions in both time dimensions, zero order baseline corrections in both dimensions, and obtained relaxation times for a total of 138 (non-proline) residues with well resolved signals by fitting measured peak intensities to a function of the form $I = I_0 e^{-t/T_n}$, where $n = 1$ or 2. We determined the errors in T_1, and T_2 by Monte-Carlo simulations.[35] The errors in relaxation parameters, for each of the two independent data sets and averaged over all residues, are 25 and 23 ms in T_1, and 2.9 and 2.2 ms in T_2, corresponding to average errors of 3.7%, in T_1, and 2.9%, in T_2. The pairwise rmsd values (i.e., pairwise errors) for the two sets of T_1,

(23) Lipari, G.; Szabo, A. *J. Am. Chem. Soc.* **1982**, *104*, 4546−4559.
(24) Lipari, G.; Szabo, A. *J. Am. Chem. Soc.* **1982**, *104*, 4559−4570.
(25) Clore, G. M.; Szabo, A.; Bax, A.; Kay, L. E.; Driscoll, P. C.; Gronenborn, A. M. *J. Am. Chem. Soc.* **1990**, *112*, 4989−4991.
(26) Schurr, J. M.; Babcock, H. P.; Fujimoto, B. S. *J. Magn. Reson., Ser. B.* **1995**, *105*, 211−204.
(27) Tjandra, N.; Feller, S. E.; Pastor, R. W.; Bax, A. *J. Am. Chem. Soc.* **1995**, *117*, 12562−12566.
(28) Zhang, Z.; Czaplicki, J.; Jardetzky, O. *Biochemistry* **1995**, *34*, 5212−5223.
(29) Woessner, D. E. *J. Chem. Phys.* **1962**, *37*, 647−654.
(30) Woessner, D. E. *J. Chem. Phys.* **1962**, *36*, 1−4.
(31) Lee, L. K.; Rance, M.; Chazin, W. J.; Palmer, A. G. *J. Biomol. NMR* **1997**, *9*, 287−298.
(32) Wang, Y. X.; Freedberg, D. I.; Wingfield, P. T.; Stahl, S. J.; Kaufman, J. D.; Kiso, Y.; Bhat, T. N.; Erickson, J. W.; Torchia, D. A. *J. Am. Chem. Soc.* **1996**, *118*, 12287−12290.
(33) Kay, L. E.; Nicholson, L. K.; Delaglio, F.; Bax, A.; Torchia, D. A. **1992**.
(34) Grzesiek, S.; Bax, A. *J. Am. Chem. Soc.* **1993**, *115*, 12593−12594.
(35) Kamath, U.; Shriver, J. W. *J. Biol. Chem.* **1989**, *264*, 5586−5592.

T_2, and NOE measurements are 5.0%, 3.9%, and 7.7%, respectively. These pairwise errors are approximately equal to the average error for each measurement multiplied by $\sqrt{2}$, indicating that errors in the measured data arise primarily from random (Gaussian) noise. We combined the two data sets, calculating the respective T_1 and T_2 values and their average errors in the following way: $T_n(\text{av}) = [T_n(1) + T_n(2)]/2$, $\text{err}_n(\text{av}) = \sum[\text{err}_n(1) + \text{err}_n(2)]/2N$, where n=1, 2, $T_n(1)$ and $T_n(2)$ are the values of T_n in experiments 1 and 2, respectively, $\text{err}_n(1)$ and $\text{err}_n(2)$ are the errors in T_n in experiments 1 and 2, respectively, and the summation over is the total number of data sets, $N = 138$. We calculated average errors in T_1, T_2 and the NOE of 3.5%, 3.0%, and 5.5% respectively, using this procedure. In order to take account of possible small systematic errors in the relaxation measurements, we did not divide the errors by root 2, when combining the two data sets.

We measured ^{15}N $T_{1\rho}$ values on a Bruker DMX500 spectrometer for an 85% deuterated protease (except for the labile hydrogen sites) at ^{15}N and ^{1}H resonance frequencies of 50.62 and 499.53 MHz, respectively. We recorded the spectra at 45 °C with 100 and 512 complex points in the ^{15}N and ^{1}H dimensions, respectively, 64 scans per complex t1 point, spin-lock times of 4, 8, 12, 16, 24, and 32 ms, and a spin-lock field of 2.5 kHz. We found that $\langle T_{1\rho}/T_2 \rangle = 1.0 \pm 0.09$, each relaxation parameter having an average value of 97 ms. Because we were interested in measuring the short $T_{1\rho}$ values of Ile 50/150 and Gly 51/151, the maximum delay used in the $T_{1\rho}$ experiments was only 32 ms, resulting in a larger average error in $T_{1\rho}$ than in T_2.

We recorded ^{1}H$-^{15}$N NOE spectra with 1024 and 200 complex points in the ^{1}H and ^{15}N dimensions respectively, and with 64 scans per complex t1 point. We obtained ^{1}H$-^{15}$N NOE values from intensity ratio derived from two data sets taken with and without saturation of the protons. The intensities were corrected for the finite relaxation delay (2.9 s) according to published procedures.[34]

We derived H/D exchange rates from ^{1}H$-^{15}$N HSQC spectra recorded at 0.17, 0.5, 1, 2, 4, 8, 16, 24, and 48 h after initial warming of the protein solution to 34 °C in $^{2}H_2O$ solvent.[36] After recording the first spectrum with four scans per complex t1 point, we gradually increased the number of scans, reaching 64 scans for the last experiment. We measured all H/D exchange spectra with 512 and 128 complex points in the ^{1}H and ^{15}N dimensions, respectively.

Data Analysis

Extraction of Model-Free Parameters Assuming Isotropic Overall Motion. In order to calculate τ_c, we fit the relaxation data for only those residues having the ratio, T_2/T_1, within one standard deviation of the average ratio and having NOE values greater than 0.67.[18] While holding the value of τ_c constant, we allowed S^2 and τ_e to vary until the sum of residue χ^2 values reached a minimum, where

$$\chi^2 = \left(\frac{T_1(\text{exp}) - T_1(\text{calc})}{T_1(\text{error})}\right)^2 + \left(\frac{T_2(\text{exp}) - T_2(\text{calc})}{T_2(\text{error})}\right)^2 + \left(\frac{\text{NOE(exp)} - \text{NOE(calc)}}{\text{NOE(error)}}\right)^2 \quad (7)$$

and the summation, extended over residue χ^2, as given in eq 7. We then repeated the calculation, incrementing τ_c until we attained the value of τ_c that minimized the global χ^2 value. With τ_c determined in this manner, we determined S^2 and τ_e for each residue by fitting the relaxation data and minimizing χ^2 (eq 7) using the model-free approach, with $R_{ex} = 0$.[23,24] We considered the fit acceptable when $\chi^2 < 7$ because we prefer not to use additional parameters having questionable meaning in order to reduce χ^2. For residues with $\chi^2 > 7$ the relaxation data was fit using three parameters, either S^2, τ_e, and R_{ex} or S_f^2, S_s^2, and τ_s.

Model-Free Analysis in the Case of Axially-Symmetric Overall Motion. Similar to the analysis in the isotropic case, we initially excluded residues that have relaxation parameters indicating internal motion. Then, we used the T_1/T_2 ratios to determine the average correlation time, $\bar{\tau} = 1/[2D_\parallel + 4D_\perp]$, the anisotropy $\sigma = D_\parallel/D_\perp$, and the orientation (θ, ϕ) of the unique diffusion axis in the molecular (X-ray) frame. Initially, we assumed that $(\theta, \phi) = (0, 0)$, i.e., the principle diffusion axis is coincident with the z-axis of the coordinate frame of the HIV-Pr/KNI-272 crystal structure, and the angle, α_i, between each NH vector, and this axis is calculated using the X-ray coordinates. For each set of values, θ, ϕ, $\bar{\tau}$, and σ we calculated

$$E = \sum_{\text{residues}} \frac{\left(\left[\frac{T_1^{(\text{exp})}}{T_2^{(\text{exp})}}\right]^2 - \left[\frac{T_1^{(\text{pred})}}{T_2^{(\text{pred})}}\right]^2\right)}{\Delta^2} \quad (8)$$

where $[T_1^{\text{exp}}/T_2^{\text{exp}}]$ is the experimental T_1/T_2 ratio, Δ is the error in the T_1/T_2 ratio, and $[T_1^{\text{pred}}/T_2^{\text{pred}}]$ is the T_1/T_2 ratio calculated using eq 1, 2, and 5 along with the assumption that $S^2 = 1$, i.e., internal motion is neglected. We incrementally varied the above parameters until E was minimized, yielding the final values of θ, ϕ, $\bar{\tau}$, and σ.[13]

Criteria for Determining Intermonomer Differences in Order Parameters. The uncertainty in S^2 depends on the experimental errors in the measured T_1's, T_2's and NOEs. We estimated the errors in S^2 by using a Monte-Carlo[35] approach to generate 100 sets of synthetic T_1's, T_2's and NOEs, which were fitted to yield a distribution of S^2 values having an average error of 0.016. This procedure underestimates the uncertainty in S^2 because the global parameters $(\theta, \phi, \bar{\tau}, \sigma)$ are not varied in the fictitious data sets. The average pairwise S^2 rmsd of residues in monomer 1 with corresponding residues in monomer 2 is 0.037, indicating that the upper limit of average uncertainty in S^2 is 0.026. We therefore estimate that the average uncertainty in S^2 is 0.02 and consider differences in S^2 (between residues i and i + 100 in monomers 1 and 2, respectively) greater than 0.06 to be statistically significant.

Chemical Exchange. Exchange of the ^{15}N spin between two chemical environments lowers T_2 if it occurs on a time scale which is on the order of the reciprocal ^{15}N chemical shift difference of the exchange sites. In order to account for chemical exchange, we included a parameter R_{ex} to fit the T_2 data, eq 2, in cases where the simple model-free approach is unable to fit the relaxation data.

Results and Discussion

Examination of the ^{1}H$-^{15}$N HSQC spectrum of the HIV$-$Pr/KNI-272 complex, Figure 2, shows that, in many instances, an amide signal of residue (i) on monomer 1 is clearly resolved from that of residue (i + 100) on monomer 2. In general, such well resolved signals are from residues that are close to the asymmetric KNI-272 molecule, while signals that have very similar or degenerate amide chemical shifts are typically from residues that are far from the inhibitor.

Because of the good signal dispersion in the HSQC spectrum at 34 °C, we could measure relaxation parameters for 138 amide sites, and these parameters are plotted vs amino acid residue number in Figure 3. Relaxation parameters show large deviations from their average values for residues 38$-$42/138$-$142 in the flap elbows, residues 49/149 in the tips of the flaps, and residues in the N- and C-termini. In addition, as a consequence of exchange broadening, we were unable to observe signals of residues 5/105, 50/150, and 51/151, in the relaxation spectra

(36) Marion, D.; Ikura, M.; Tschudin, R.; Bax, A. *J. Magn. Reson.* **1989**, *85*, 393$-$399.

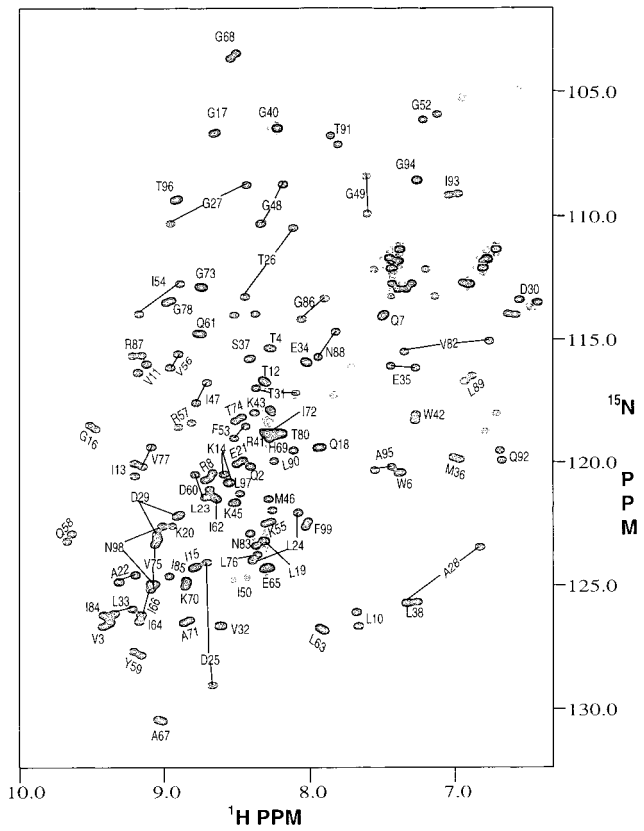

Figure 2. $^1H-^{15}N$ HSQC spectrum of the HIV-Pr/KNI-272 complex illustrating the different chemical shifts observed for the two monomers. Monomer-specific assignments are tabulated elsewhere.[37] Negative peaks appearing as broken lines are due to aliased Arg side-chain NH's, and unlabled positive peaks are due to Gln and Asn side-chain NH's. ^{15}N and ^{13}C chemical shifts are indirectly referenced with respect to liquid ammonia[46] and to TSP,[47] respectively.

recorded at 34 °C. At 45 °C, we observed signals for residues 50/150 and 51/151 and, although they were broad and weak, were able to measure their $T_{1\rho}$ values.

In order to extract motional parameters from the relaxation data, we first applied the model-free formalism in its simplest form, i.e., assuming that overall motion is isotropic. Using procedures outlined in the Theory section, our analysis yields $\tau_c = 9.5$ ns (data not shown), in good agreement with previous measurements.[12,13] The S^2 values vary from 0.55 to approximately 0.98. Although these are physically reasonable values for S^2, it was found that 23 residues required a nonzero R_{ex} value and six data sets required the extended model-free[25] treatment in order to achieve $\chi^2 \leq 7$. Furthermore, 15 data sets could not be fit with any of the isotropic models discussed above. These results suggest that the assumption of isotropic reorientation is not justified, in agreement with Tjandra et. al.[13] who have recently shown that when the HIV-Pr/DMP323 complex is treated as a nonspherical rotor, relaxation data for residues Thr 31, Asp 60, Ile 62, and Thr 80 are well fit using the simple model-free form for $J(\omega)$, eq 4. In contrast these residues require an exchange contribution, $R_{ex} > 0$, when fit assuming isotropic overall reorientation.[12] These residues have below-average T_2's because their amide NH bonds make small angles with the longest diffusion axis of the HIV-Pr/DMP323 complex and not because of chemical exchange, as was previously thought.

Further evidence indicating a need for an anisotropic analysis of the relaxation data for the HIV-Pr/KNI-272 complex is

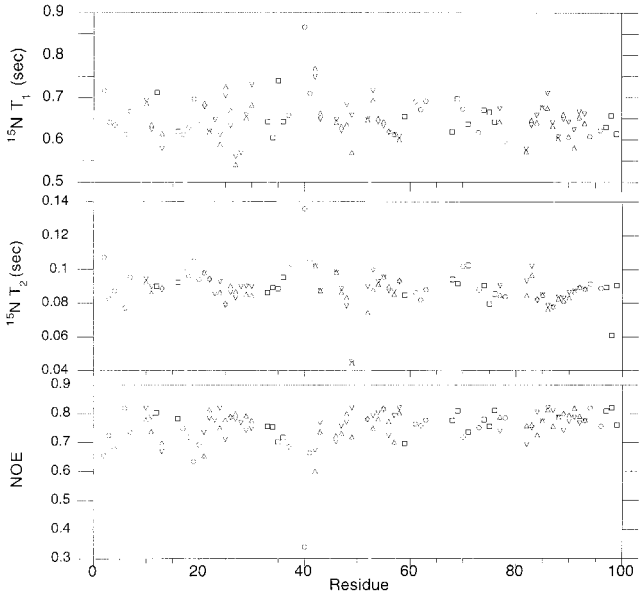

Figure 3. A comparison of backbone amide ^{15}N T_1, T_2, and NOE vs amino acid residue obtained for the two monomers of the HIV-protease/KNI-272 complex. The results shown are the average of two independent data sets, and the average errors in the parameters are 3.5%, 3.0%, and 5.5%, respectively. Down-pointing triangles correspond to residues assigned to monomer 1, the up-pointing triangles correspond to residues assigned to monomer 2, and the circles correspond to residues with degenerate chemical shifts. NH's having nondegenerate chemical shifts, but not assigned to a specific monomer, are arbitrarily numbered i or i + 100.

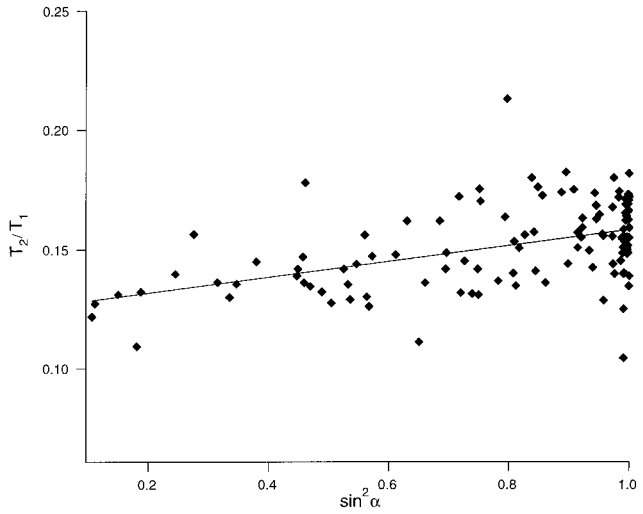

Figure 4. The T_2/T_1 ratio plotted vs $\sin^2 \alpha$, where α is the angle made by the amide N−H bond vector and the unique (Z) principal inertial axis. The T_2/T_1 data are fit to the eq 6, and the slope of the fitted line yields an anisotropy of 1.34.

provided in Figure 4, which shows a good linear fit of T_2/T_1 to $\sin^2 \alpha$, as predicted by eq 6 for an axially symmetric rotor. From the slope and intercept of the fit in Figure 4, it is found that $D_{||}/D_{\perp} = 1.34$ and $\bar{\tau} = 9.6$ ns.

We carried out a more exact determination of these parameters using the computational approach of Tjandra and Bax, described in Data Analysis, which yielded the following results: $\bar{\tau} = 9.65$ ns, $D_{||}/D_{\perp} = 1.27$, $\theta = 7.25$, $\phi = 163°$. As expected, we obtain values of $D_{||}/D_{\perp}$ and $\bar{\tau}$ similar to those derived from the approximate analysis, because the correlation time and anisotropy are in the range where eq 6 is a good approximation. Not surprisingly, the results are similar to those

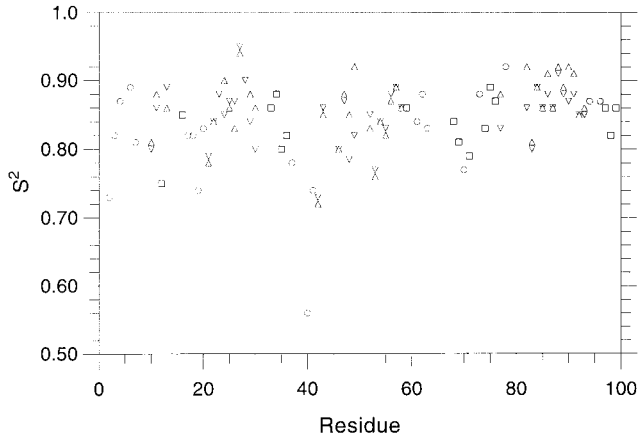

Figure 5. Backbone amide S^2 values vs amino acid residue number in the HIV-protease/KNI-272 complex obtained assuming anisotropic protein diffusion with $\langle\tau\rangle = 9.65$ ns and $D_{||}/D_{\perp} = 1.27$. The down-pointing triangles correspond to residues assigned to monomer 1, the up-pointing triangles correspond to residues assigned to monomer 2, and the circles correspond to residues with degenerate chemical shifts. S^2 values for NH's having nondegenerate chemical shifts, but not assigned to a specific monomer, are averaged and plotted as squares.

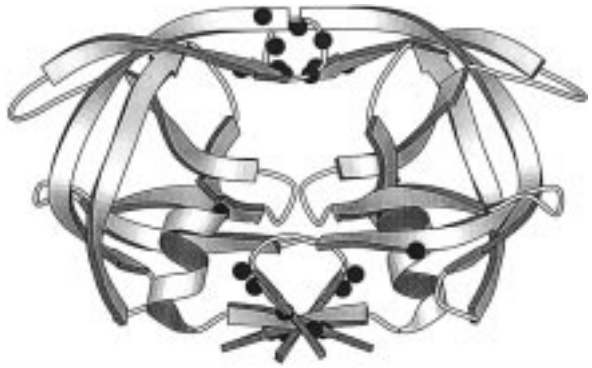

Figure 6. MOLSCRIPT[48] diagram of HIV protease backbone, with spheres at the positions of amide residues that require a conformational exchange term to fit their relaxation data. These residues are clustered near the tips of the flaps (Gly 48/148, Gly 49/149, Ile 50/150, Gly 51/151, Gly 152, Phe 153, at the top of the drawing) and the N-terminal loop and four-stranded β-sheet (Val 3/103, Thr 4/104, Leu 5/105—the latter not observed in the NMR spectra, presumably due to conformational exchange—Trp 6/106, Arg 87/187, and Asn 98/198, at the bottom of the drawing.) Flexibility of the flap tips and the N-terminal loop are thought to modulate HIV protease function.

obtained from the analysis of HIV-Pr/DMP323[13] relaxation data, since the DMP323 and KNI-272 complexes have similar overall shapes. The order parameters obtained for the KNI-272 complex, assuming anisotropic reorientation (Figure 5) have an average value of 0.85. More significantly, only seven residues require an R_{ex} contribution, none require the extended model-free formalism[25] to fit the relaxation, and one residue cannot be fit, when anisotropic reorientation is assumed. Residues undergoing ms time scale motion are indicated in Figure 6 by black spheres. Finally, we note that residues 67/167/95/195 have been excluded from our analysis, because they are Ala residues in the protease studied herein but are Cys residues in the protease used in the X-ray study. Hence, the values of the angle α derived from the crystal structure may not be appropriate for the analysis of the relaxation data. A comparison of parameters obtained from the isotropic and anisotropic analysis of relaxation data is given in Table 1.

Table 1. Comparison of Global Parameters To Use Fit the Relaxation Data

model	$D_{||}/D_{\perp}$	θ (deg)	ϕ (deg)	τ (ns)	av S^2
isotropic rotor	1			9.5	0.84
axially symmetric rotor	1.27	7.25	163	9.65	0.85

Internal Motion in the HIV-Pr/KNI-272 Complex. The values of S^2 for both monomers are plotted as a function of residue number in Figure 5. The S^2 values of monomers 1 and 2 are indicated by down-pointing and up-pointing arrows, respectively; the S^2 for residues where monomer-specific assignments are not available are averaged and marked with a square, while S^2 of NH's having degenerate chemical shifts are indicated by a circle.[37] We observe the smallest order parameters, in the range from 0.56 to 0.79, for residues 37-42/137-142 in the flap elbows. In addition, their amide hydrogens exchange quickly with bulk solvent, an observation which is consistent with rapid, large-amplitude motions and their location on the protein surface. Molecular dynamics simulations of the HIV-Pr/KNI-272 complex reveal S^2 values in agreement with those obtained by NMR,[38] and residues in the flap elbows have large crystallographic *B*-factors.[39] Finally, it has been shown that nonconservative replacement of Leu 38 diminishes protease activity.[40] Taken together, these results enforce the conclusion that the flap elbows are highly flexible, and their flexibility may be important for function.[40]

In contrast with residues in the elbows of the flaps, the remaining residues in the flap region, residues 46−49/52−56/146−149/152−156 have order parameters in the range of 0.8−0.9, indicating they are relatively well ordered with small amplitude motions in the ns-ps time scale. One exception to this statement is observed in the case of the residue pair 53/153, which have order parameters of 0.77/0.76. In addition a chemical exchange term is required to fit the relaxation parameters of Gly 152 and Phe 153 but not of Gly 52 and Phe 53.

We were unable to measure relaxation parameters of Ile 50/150 and Gly 51/151 at 34 °C because their line widths were so large that their amide signals were barely observable in HSQC spectra. At 45 °C, we did observe their signals in HSQC spectrum, but compared with typical amide signals they had low intensity and were noticeably broadened in the ^{15}N dimension. These observations indicate that Ile 50/150 and Gly 51/151 have depressed $T_{1\rho}$ and T_2 values due to chemical exchange. This hypothesis is confirmed by $T_{1\rho}$ measurements, which show that these residues have $T_{1\rho}$ values of ca. 20 ms, nearly 5-fold smaller than the average $T_{1\rho}$ found for other residues in the protein at 45 °C. In addition, H_N-H_N NOEs from a NOESY spectrum of the HIV-Pr/KNI-272 complex (85% perdeuterated protein, mixing time 250 ms) show evidence for a mixture of a β-I type turn and a β-II type turn for both monomers at the tips of the flaps, in contrast to the unique conformation seen in the crystal. Hence the NOE patterns and depressed $T_{1\rho}$'s support a model in which β-I and β-II type turns interconvert at the tips of the flaps on the millisecond time scale.[12] It has been noted that such a conformational interconversion preserves the hydrogen bonds donated by Ile 50/150

(37) Wang, Y. X.; Freedberg, D. I.; Yamazaki, T.; Wingfield, P. T.; Stahl, S. J.; Kaufman, J. D.; Kiso, Y.; Torchia, D. A. *Biochemistry* **1996**, *35*, 9945−9950.
(38) Lu, X.; Collins, J. *J. Am. Chem. Soc.* **1998**, submitted.
(39) Baldwin, E. T.; Bhat, T. N.; Gulnik, S.; Liu, B.; Topol, I. A.; Kiso, Y.; Mimoto, T.; Mitsuya, H.; Erickson, J. W. *Structure* **1995**, *3*, 581−590.
(40) Loeb, D. D.; Swanstrom, R.; Everitt, L.; Manchester, M.; Stamper, S. E.; Hutchison, C. A. I. *Nature* **1989**, *340*, 397−400.

amides, and studies of HIV-Pr kinetics show that chemical replacement of Ile 50/150 with moieties incapable of donating a hydrogen bonds results in an inactive enzyme.[41] Taken together, these results suggest that tips of the flaps form a dynamic hydrogen bond structure that stabilizes the protease, yet permits flexibility required for product release from the active site.

The Binding Site of the Protease. The residues forming part of the KNI-272 binding site (22−30/122−130) are well ordered, as indicated by their relatively large order parameters, with Gly 27/127 showing the highest order parameters in the molecule, 0.95 and 0.94, respectively. Furthermore, the H/D exchange data show that the exchange rates of the amide NH's of residues 22−28/122−128 are on the order of days. In contrast to the HIV-Pr/DMP323 complex,[12,13] we find no evidence for motion on the micro- to millisecond time scale for the NH's of Asp 25/125 in the HIV-Pr/KNI-272 complex, suggesting that these residues reside in a more rigid environment in the latter complex. The order parameters for residues 22−30 are in good agreement with those calculated from the MD simulations.[38]

Dynamics in Other Regions of the Protease. Residues 17−21 have smaller than average order parameters but larger than those in the flap elbows. MD studies of HIV-Pr show that this region is flexible,[8,38] with average order parameters ca. 0.05 less than those determined by NMR. It has been proposed that this region of the molecule acts as a molecular lever, raising the elbows and ultimately opening the flaps.[9,10] Although the NMR data do not speak to this issue, chemically synthesized HIV-Pr, in which this loop is rigidified, retains WT activity, showing that the flexibility of this loop is not related to catalysis.[42]

Residues in the four-stranded β-sheet made by the N- and C-termini of the two monomers, Val 3/103, Thr 4/104, Ala 95/195, Thr 96/196, Leu 97 (or 197), Asn 98/198, and Phe 99/199, have large order parameters, indicating that they undergo only small amplitude motions on the ns-ps time scale. Gln 2/102 (degenerate chemical shifts) have smaller than average order parameters, 0.73, a result that correlates with the observations that the NH's of these residues do not contribute hydrogen bonds to the sheet and exchange readily with solvent. In contrast, the amides of Val 3/103 and Asn 98/198 have large order parameters, are in slow exchange with solvent, and donate hydrogen bonds in the β-sheet.[39] Hence it is difficult to argue that these residues undergo large amplitude slow motions in order to explain the observation that an R_{ex} contribution is required to fit their relaxation data. An alternate possibility[12] is that the motion of the loop containing residues Thr 4/104, Leu 5/105, and Trp 6/106 modulates the chemical shifts of the nearby Val 3/103 and Asn 98/198 amides, increasing their line widths, although these latter residues are not themselves mobile.[12] The motion of the loop is thought to broaden and severely attenuate the Leu 5/Leu 105 signals and may play a role in autoproteolysis, since the prime autolysis site in the protein is the Leu 5-Trp 6 peptide bond.[40,43]

Comparison of Internal Dynamics of the Two Monomers. A comparison of the order parameters of residue (i) in monomer 1 with residue (i + 100) in monomer 2, Figure 7, shows only residues Gly 49/149, whose order parameters are 0.82 and 0.92, respectively, have a difference in order parameters greater than $2p_{sd}$ (p_{sd} (0.03) is the pairwise rmsd calculated based upon the standard error in S^2 of 0.02). The larger order parameter observed for Gly 149 may be related to the observation that the carbonyl carbon of Gly 148 and amide proton of Ile 150 participate in the hydrogen bond network formed by the protein, KNI-272, and several bound water molecules in the crystal structure.[39] Although the NH of Ile 50 is part of this network, the carbonyl of Gly 48 is not. Hence, the NMR observation that NH of Gly 149 is more constrained than is the NH of Gly 49 correlates with the H-bonding observed in the crystal structure. We also find that S^2 for Gly 148 is 0.06 larger than S^2 of Gly 48. The order parameter of residues 129 and 182 are also 0.06 larger than those of 29 and 82, respectively. In the crystal structure,[39] the NH of Asp 129 and the CO of Gly 127 hydrogen bond directly to the backbone of KNI-272, whereas the NH of Asp 29 and the CO of Gly 127 hydrogen bond to a bound water molecule. The water molecule is in fast exchange on the chemical shift time scale, whereas the inhibitor is not, suggesting that the Asp 129 hydrogen bond is more stable that that of Asp29.[32] Hence, the differences in the order parameters of Asp29/129 and Gly48/148 appear to correlate with the crystal structure. However, since the order parameter differences for these residues are only $2p_{sd}$, they are at the margin of statistical significance, and hence, these correlations of S^2 differences with structure, while interesting, must be regarded as tentative.

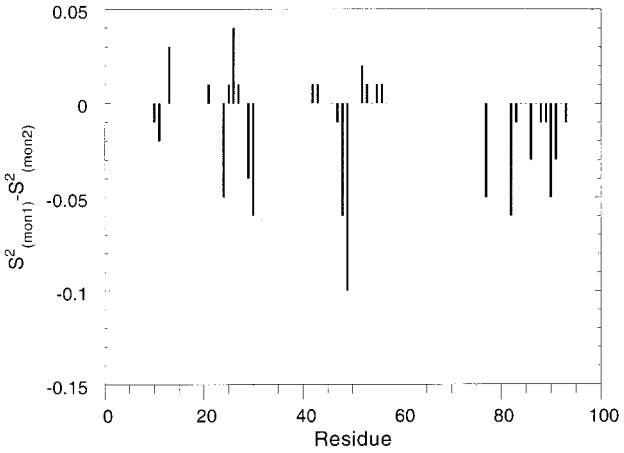

Figure 7. Plot summarizing the differences in order parameters of amides in the two HIV protease monomers, S^2(monomer 1) − S^2(monomer 2), as a function of the residue number.

In addition to indicating differences in S^2 for specific residue pairs in the two monomers, Figure 7 also suggests that, overall monomer 2 is more ordered than monomer 1. It is interesting to compare the relative flexiblity of the two monomers in solution with the *B* factors determined from the crystal structure.[39] Because the *B* factor is a measure of disorder in the crystal, we compare B(1)−B(2) with A(1)−A(2), where 1 and 2 refer to monomer 1 or 2, respectively, and $A = 1 - S^2$. Note that A is a measure of flexibility in solution and is related to the rms angle of the NH bond axis fluctuation. For example, using a "wobble in a cone" to model the motion of the NH vector, A is proportional to the square of the cone semiangle.[23,24] A comparison of A(1)−A(2) with B(1)−B(2) is seen in Figure 8. While there is not a residue-specific correlation of A(1)−(2) and B(1)−B(2), the plots of these differences vs residue number, Figures 8a,b, both indicate that monomer (1) is more flexible than monomer (2). Figure 8a shows that A(1)−A(2) > p_{sd} for eight residues, whereas A(2)−A(1) > p_{sd} for only one residue, while in Figure 8b, B(1)−B(2) > 5 Å^2 for six residues, whereas B(2)−B(1) > 5 Å for a single residue. Hence,

(41) Baca, M.; Kent, S. B. H. *Proc. Natl. Acad. Sci. U.S.A.* **1993**, *90*, 11638−11642.
(42) Baca, M.; Alewood, P. F.; Kent, S. B. H. *Protein Sci.* **1993**, *2*, 1085−1091.
(43) Rosé, J. R.; Salto, R.; Craik, C. S. *J. Biol. Chem.* **1993**, *268*, 11939−11945.

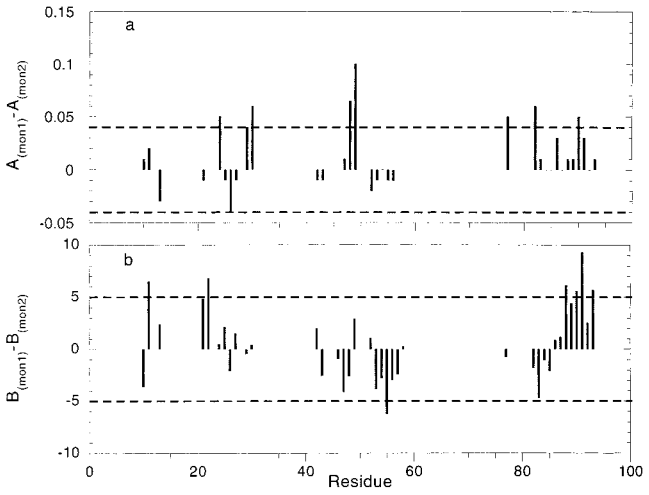

Figure 8. Comparison of the differences in (a) the NMR order parameters, expressed as A(monomer 1) − A(monomer 2), where A $= 1 - S^2$ with (b) the differences in the X-ray *B*-factors for the backbone atoms, *B*(monomer 1)−*B*(monomer 2), plotted as a function of residue number. The dashed lines in (a) a drawn at a level of $\pm p_{sd}$, where p_{sd} is the pairwise rmsd calculated using the estimated error of 0.02 in S^2. In (b) the dashed lines are drawn at a level of ±5 Å^2.

it appears that binding to the asymmetric inhibitor induces some difference in the overall internal flexibility of the two protease monomers.

In addition to differences in the amplitudes of the motions between the two protease monomers, the analysis also indicates a few sites where the time scales of the motion may differ. Evidence that motion on the chemical exchange time scale affects spin relaxation is found for Gly 152 and Phe 153 (although R_{ex} is small for Phe 153) but not for Gly 52 and Phe 53. We cannot be certain that the motion of these residues themselves is responsible for the R_{ex} contribution to their relaxation, because slow motion at the tips of the flaps involving residues 49−51/149−151 may modulate the chemical shfits of residues 52−53/152−153. It is, however, interesting to note that the aromatic ring of Phe 153 loosely packs against the isoquinoline ring of the inhibitor,[39] whereas Phe 53 is not close to the inhibitor.

Conclusions

This study of the HIV-Pr/KNI-272 complex continues our investigation of the backbone dynamics of complexes of HIV-Pr with potent inhibitors, having K_i's ranging from ca. 10 nM to 5 pM. Our results show that the backbone of the HIV-Pr is well ordered, with most residues having order parameters in the range of 0.8−0.95. Since this result is essentially independent of the inhibitor K_i it is likely to apply generally to potent inhibitors having K_i values less than 10 nM. The order parameters measured for the KNI-272 complex correlate well with those calculated by the MD simulation.[38]

Although most of the backbone of the inhibited protease is highly ordered, several segments of the polypeptide chain are flexible. Nearly all of the residues that experience motion on the chemical exchange time scale are concentrated in either the tips of the flaps or are near the terminal loop containing residues 4/104−6/106. It is interesting that the residues in the tips of the flaps are flexible on the chemical exchange time scale in all three complexes studied, yet these residues contribute hydrogen bonds that stabilized the structure of the complex. Hence, the tips of the flaps appear to have a dual role: they stabilize the complex yet have the flexibility to facilitate product release following catalysis. The flexibility observed in the N-terminal loop, residues 4−6, may be related to autoinactivation of the protease, since this is the prime autocatalysis site in the protein.

The presence of several flexible segments in the backbone of the inhibited protease suggests that the polypeptide backbone of the free protein may be highly mobile. The recent availability of an autolysis resistant, but fully active mutant protease,[43,44] has opened the way to compare the dynamics of the free and inhibited proteins by NMR methods.[7]

The difference in order parameters found for Gly 49/149 (and possibly Gly 48/148 and Asp29/129) amide NH's in the protease/KNI-272 complex correlates with differences in their inhibitor interactions in the crystal structure. Moreover, we find overall flexibility is greater in monomer 1 than in monomer 2, suggesting that the flexibility of the polypeptide backbone is somewhat sensitive to differences in interactions with an asymmetic ligand. In order to further investigate protease/inhibitor interactions we plan to study the side-chain dynamics at the ligand binding site of the protease, which contains numerous large hydrophobic side chains whose flexibility should be more sensitive interactions with protease ligands than the backbone. Hence, new approaches[45] for studying the flexibility of methyl groups in proteins have the potential to yield novel information about protease/inhibitor interactions and about the flexibility of the ligand binding site in the free protease as well.

Acknowledgment. We thank Frank Delaglio for nmrPipe, nmrDraw, and additional software, Dan Garrett for PIPP, Jack Colllins, Rieko Ishima, Nico Tjandra, and Andy Hinck for useful discussions. This work was supported by the AIDS Targeted Anti-Viral Program of the Office of the Director of the National Institutes of Health.

JA981206R

(44) Mildner, A. M.; Rothrock, D. J.; Leone, J. W.; Bannow, C. A.; Lull, J. M.; Reardon, I. M.; Sarcich, J. L.; Howe, W. J.; Tomich, C.-S. C.; Smith, C. W.; Heinrikson, R. L.; Tomaselli, A. G. *Biochemistry* **1994**, *33*, 9405−9413.

(45) Muhandiram, D. R.; Yamazaki, T.; Sykes, B. D.; Kay, L. E. *J. Am. Chem. Soc.* **1995**, *117*, 11536−11544.

(46) Live, D.; Davis, D. G.; Agosta, W. C.; Cowburn, D. *J. Am. Chem. Soc.* **1984**, *106*, 1939−1941.

(47) Bax, A.; Subramanian, S. *J. Magn. Reson.* **1986**, *67*, 565−569.

(48) Kraulis, P. *J. Appl. Cryst.* **1991**, *24*, 946−950.